# SUPPORTING INFORMATION

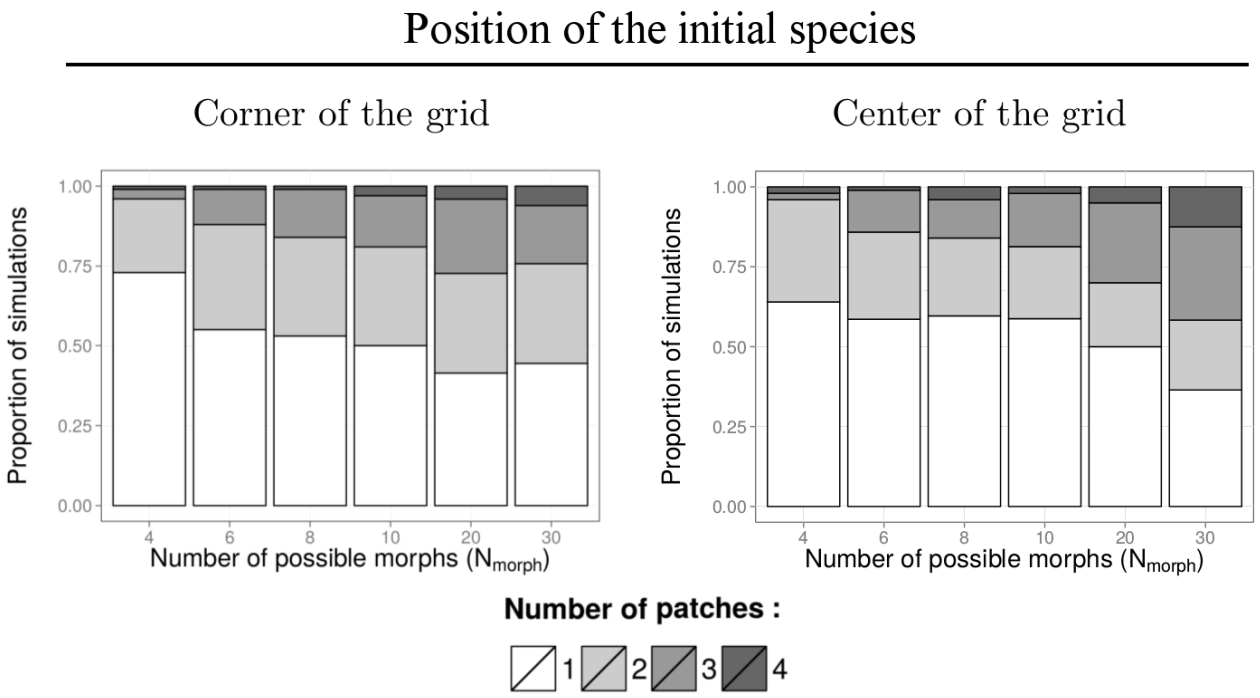


Figure S1: Formation of the spatial mosaic of morphs. We plot the proportion of simulations resulting in mosaics with different numbers of patches (represented by different shades of grey) under two different starting conditions: when the initial species is placed at the corner or at the center of the grid. Parameter values: see Table 1. $s_c = 0.50$.
*The results are qualitatively similar and the formation of the mosaic is possible whatever the position of the initial species. Therefore, the position of the initial species does not matter.*

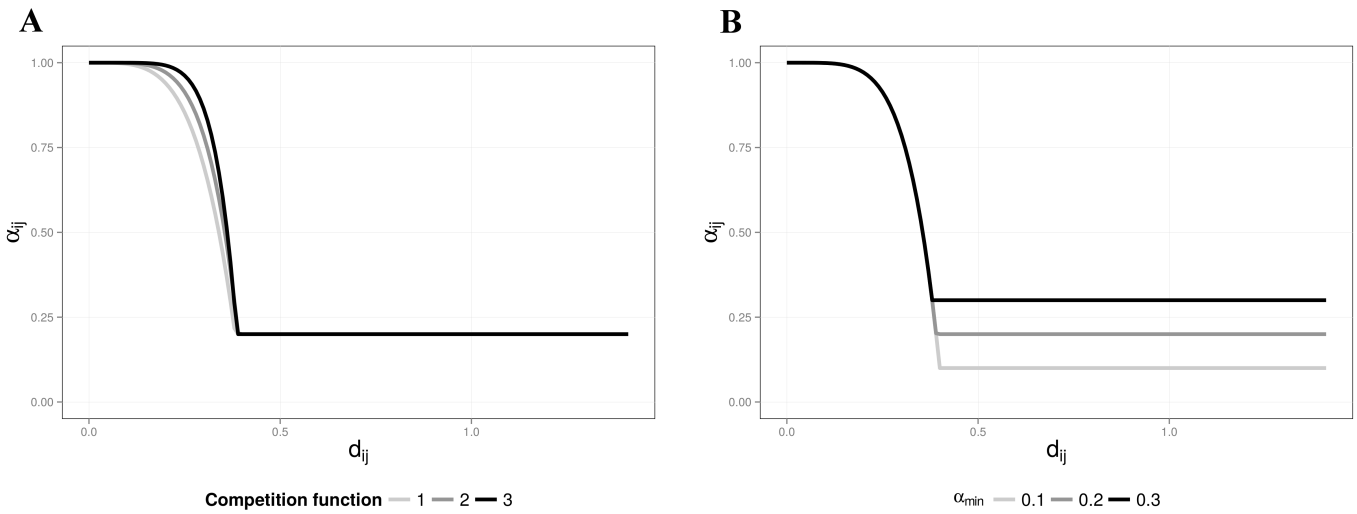


Figure S2: Competition term $\alpha_{ij}$ calculated from the Euclidean distance $d_{ij}$ between positions $(x_i, y_i)$ and $(x_j, y_j)$ of two species in the ecological space. The curves are drawn with different values of $(f, C)$ (A) or of minimum competition term possible $\alpha_{\min}$ (B). In subfigure A, the competition functions 1, 2 and 3 correspond to the competition functions with parameters $(f, C)$ : $(4, 150)$, $(5, 500)$ and $(7, 7000)$, respectively. The default values of $(f, C)$ and $\alpha_{\min}$ implemented in our study are $(5, 500)$ and 0.2, but other values are tested in complementary simulations (see figure S5, S13 and S14).

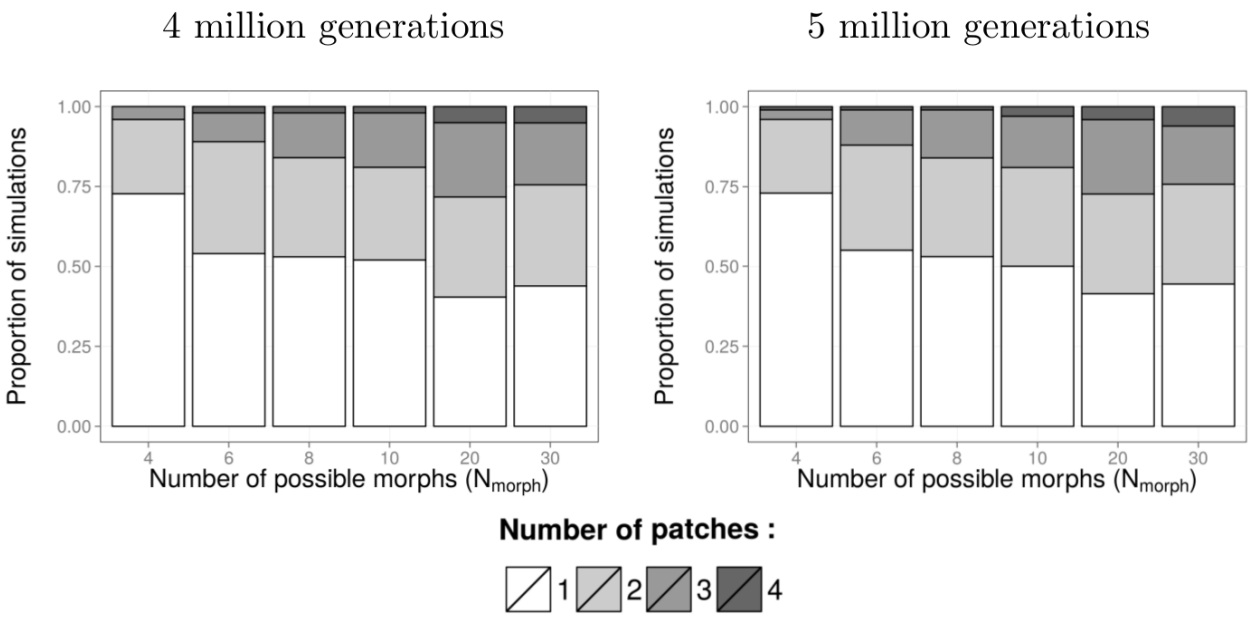


Figure S3: Formation of the spatial mosaic of morphs. We plot the proportion of simulations resulting in mosaics with different numbers of patches (represented by different shades of grey): after 4 million and after 5 million generations. Parameter values: see Table 1. $s_c = 0.50$.
*The results are qualitatively similar after 4 and 5 million generations. Therefore, our simulations allow sufficient time for equilibrium to be reached.*

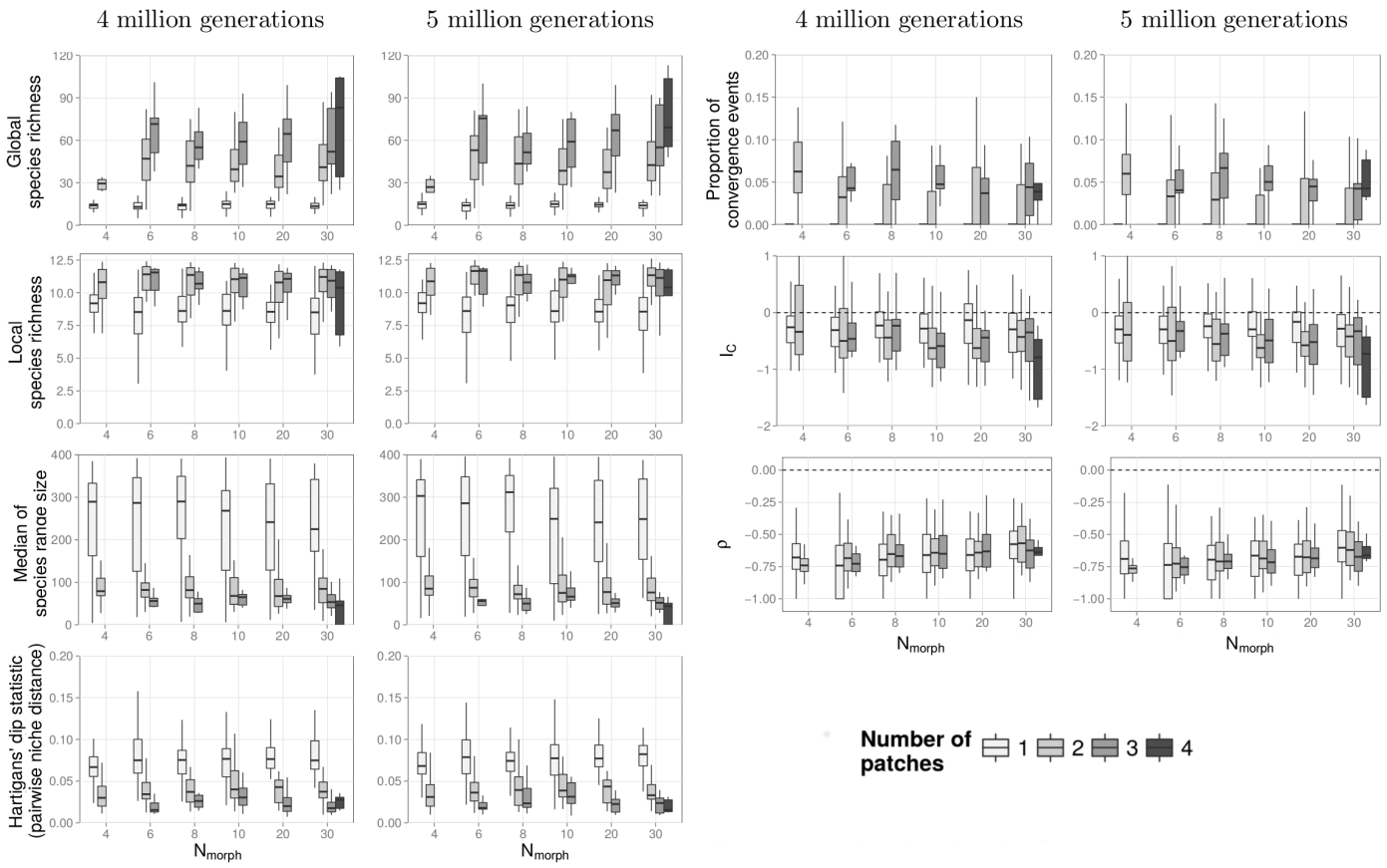


Figure S4: Relationship between the number of patches of the mosaic emerging from the simulations, the spatial and ecological structure of the prey community and the reconstructed phylogeny. Effects of the number of possible morphs ($N_{\text{morph}}$). From top to bottom, we plot the diversity of the simulated clades (global and local species richnesses), the geography of species (median of species range size), species niche occupation (Hartigans' dip statistic of the distribution of pairwise niche distance), the proportion of convergence events, the estimator of the imbalance $I_{\text{C}}$ of the resulting trees using Colless' index, and the temporal shift in diversification rate $\rho$. We record the community state and the phylogeny at two different time steps: after 4 million and after 5 million generations. For each combination of parameters, simulations are classified according to the number of patches of their resulting mosaics (different shades of grey). Data distribution is represented by box-and-whiskers plot. Parameter values: see Table 1. $s_c = 0.50$.
*The results are qualitatively similar after 4 and 5 million generations. Therefore, our simulations allow sufficient time for equilibrium to be reached.*

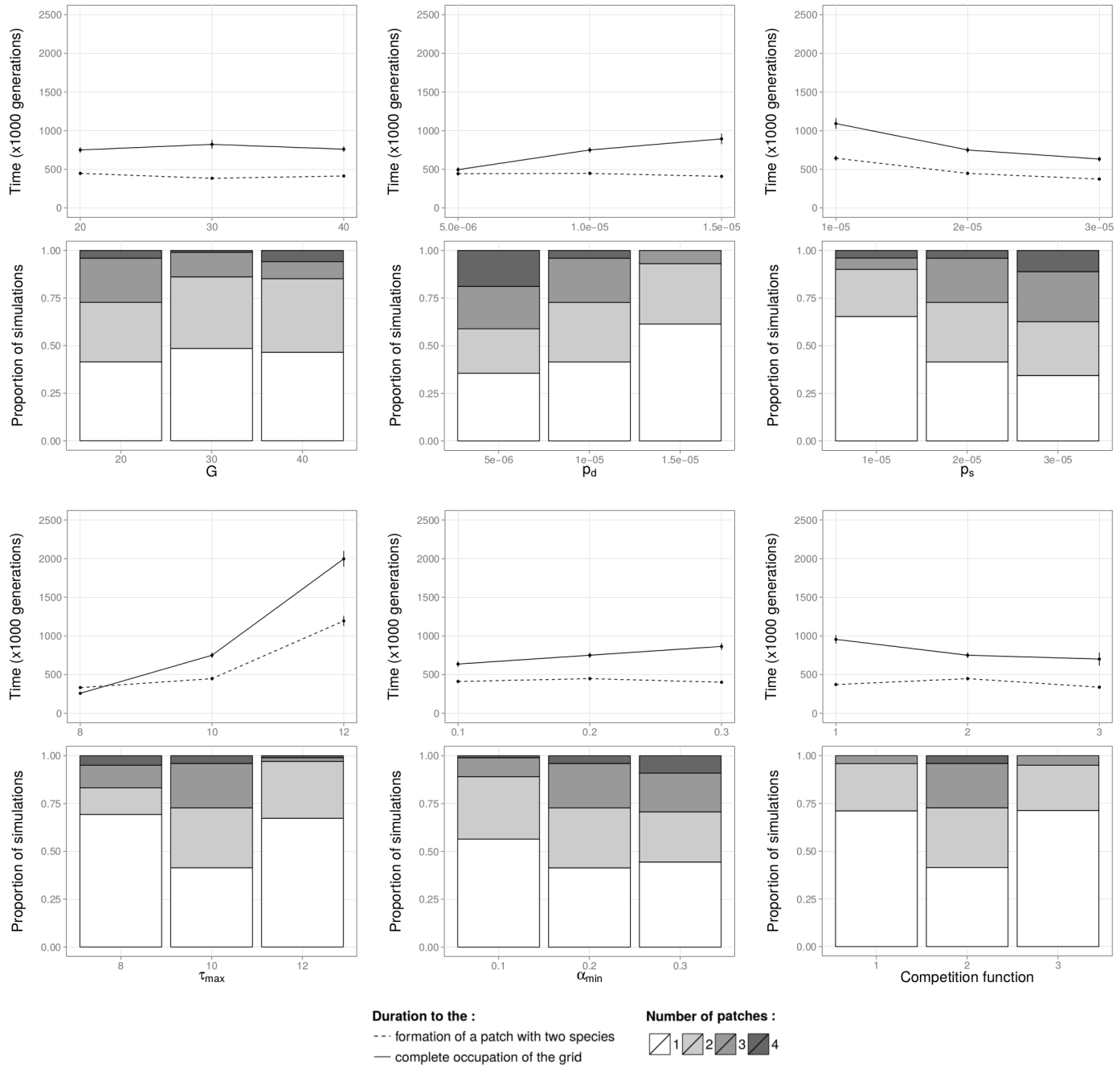


Figure S5: Formation of the spatial mosaic of morphs. Effects of the grid size ($G$), the probability of cell destruction in any given cell ($p_d$), the probability of speciation of each species in any given cell ($p_s$), the number of prey attacked before predation on a given morph ceases ($\tau_{\max}$), the minimum competition term possible ($\alpha_{\min}$), and the competition function (see figure S2A). At the top, we plot the duration to the formation of the first patch with two species and the duration to the complete occupation of the grid. At the bottom, we plot the proportion of simulations resulting in mosaics with different numbers of patches (represented by different shades of grey) after 5 million generations. Other parameter values: see Table 1.
*The formation of the mosaic is very sensitive to parameters affecting the effective speciation rate with colour shift and the effective speciation rate without colour shift, the value of which greatly affects the speed of invasion of the grid. See Fig S10 to S14 for details.*

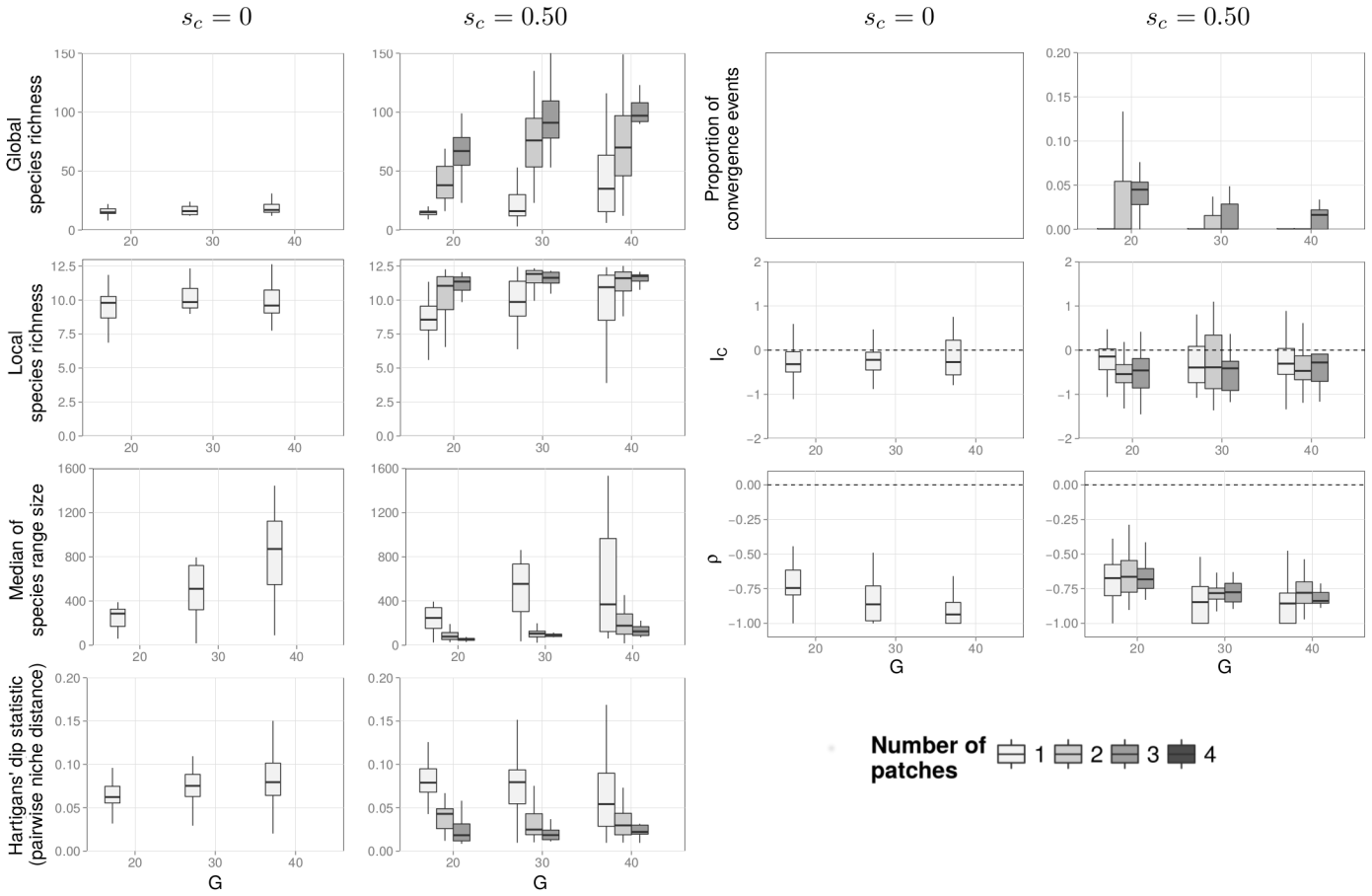


Figure S6: Relationship between the number of patches of the mosaic emerging from the simulations, the spatial and ecological structure of the prey community and the reconstructed phylogeny. Effects of the **grid size** (**G**). From top to bottom, we plot the diversity of the simulated clades (global and local species richnesses), the geography of species (median of species range size), species niche occupation (Hartigans' dip statistic of the distribution of pairwise niche distance), the proportion of convergence events, the estimator of the imbalance $I_{\mathrm{C}}$ of the resulting trees using Colless' index, and the temporal shift in diversification rate $\rho$. For each combination of parameters, simulations are classified according to the number of patches of their resulting mosaics (different shades of grey). Data distribution is represented by box-and-whiskers plot. Parameter values: see Table 1.
*We implement a grid size* $G = 20$ *in our simulations, and doubling the grid size does not affect much the output. We only observe more species in general, and we record less convergence events since the perimeter/area ratio declines as the species ranges increase.*

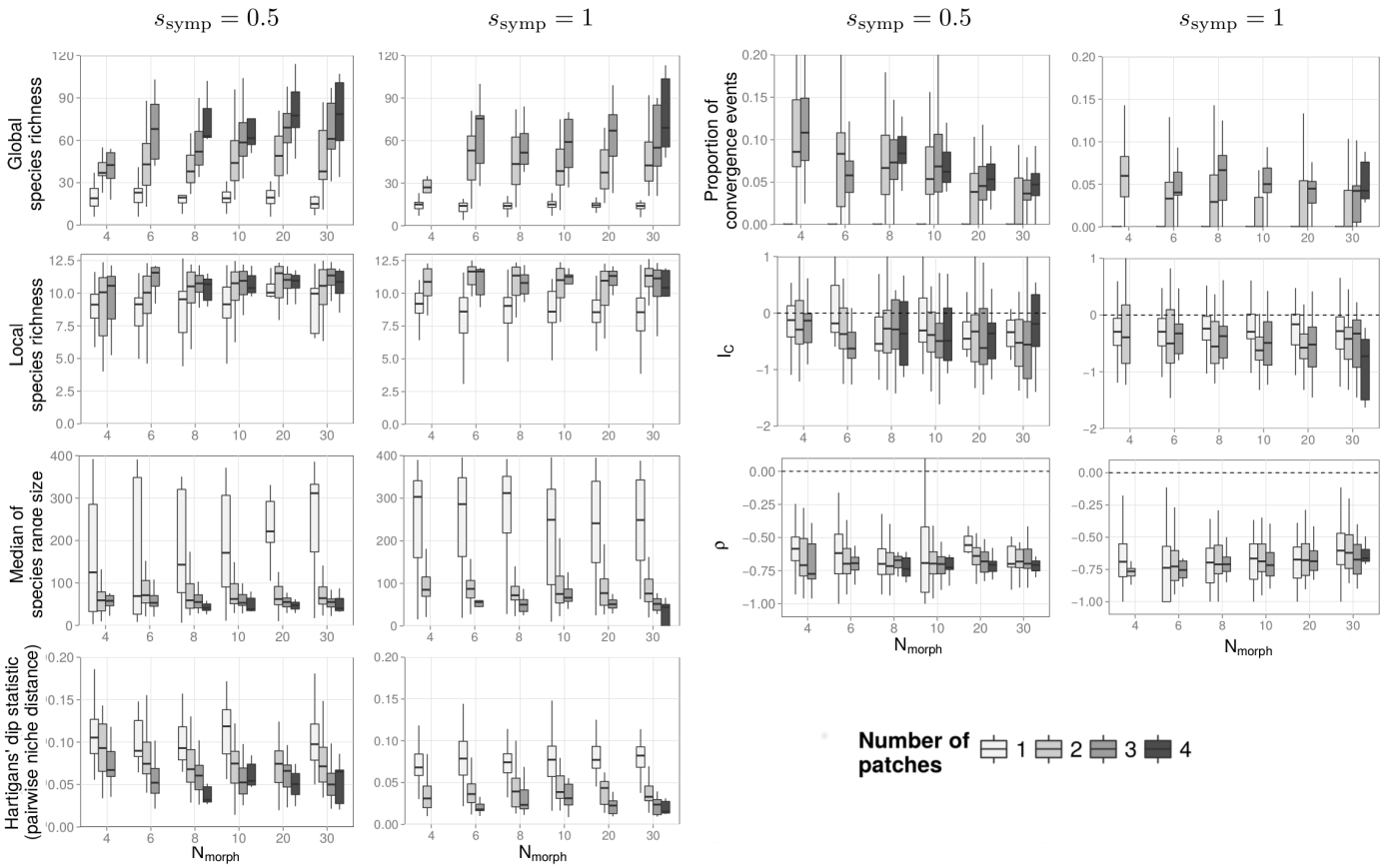


Figure S7: Relationship between the number of patches of the mosaic emerging from the simulations, the spatial and ecological structure of the prey community and the reconstructed phylogeny. Effects of the **proportion of speciation in sympatry**. From top to bottom, we plot the diversity of the simulated clades (global and local species richnesses), the geography of species (median of species range size), species niche occupation (Hartigans' dip statistic of the distribution of pairwise niche distance), the proportion of convergence events, the estimator of the imbalance $I_C$ of the resulting trees using Colless' index, and the temporal shift in diversification rate $\rho$. For each combination of parameters, simulations are classified according to the number of patches of their resulting mosaics (different shades of grey). Data distribution is represented by box-and-whiskers plot. Parameter values: see Table 1. $s_c = 0.50$.

*The formation of the mosaic is more likely when speciation can be allopatric (Fig. S9), because the effective speciation rate with colour shift is higher. This effect of allopatric speciation on the spatial mosaic affects the macroevolutionary pattern (higher species richnesses, smaller species ranges, more balanced phylogenies, more convergence events observed, when the number of patches is high). Moreover, since there are less shifts in ecological niche (we assumed that allopatric speciation is not associated to ecological shift), the occupation of the ecological niche is also less even.*

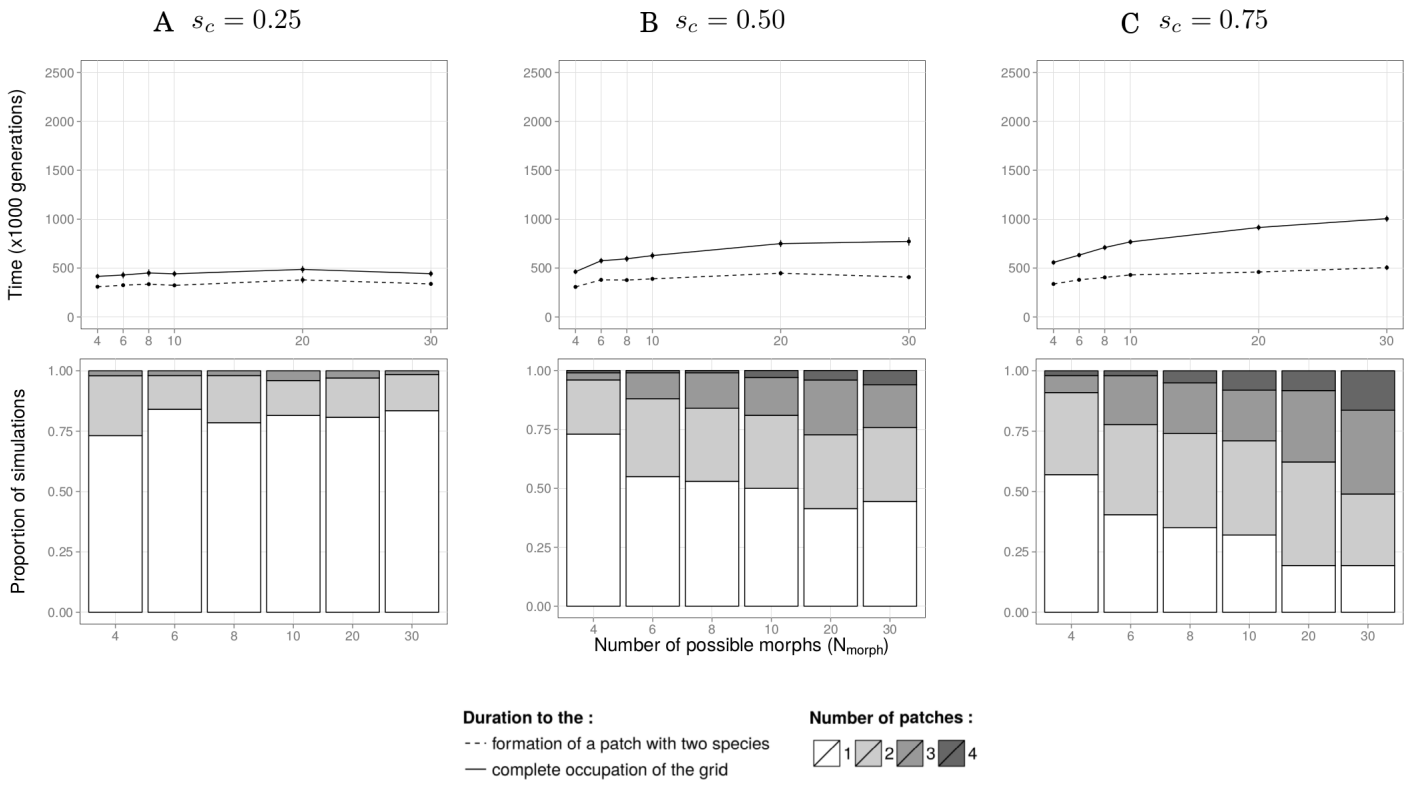


Figure S8: Effect of the number of possible morphs ($N_{\text{morph}}$) on the formation of the spatial mosaic of morphs, when there is predation, and when colour shift is implemented (values tested: $s_c = 0.25$, $s_c = 0.5$, $s_c = 0.75$). We plot the numbers of generations until the formation of the first patch with two species and until the complete occupation of the grid (represented by mean values and their confidence intervals) (at the top), and the proportion of simulations leading to different numbers of patches in the mosaic (represented by different shades of grey) after 5 million generations (at the bottom). Parameter values: see Table 1.
*When $s_c$ is high (B, C, such as in Fig. 2B), low values of $N_{morph}$, which confer a high probability of convergence, can inhibit the formation of patchy mosaics. When $s_c$ is low (A), the formation of a spatial mosaic with more than two patches is unlikely. Indeed, low $s_c$ favours the emergence of a patch with two coexisting species and a rapid invasion of the grid, limiting the formation of a mosaic. Under such conditions, there is no effect of $N_{morph}$ on the patchiness of the resulting mosaic.*

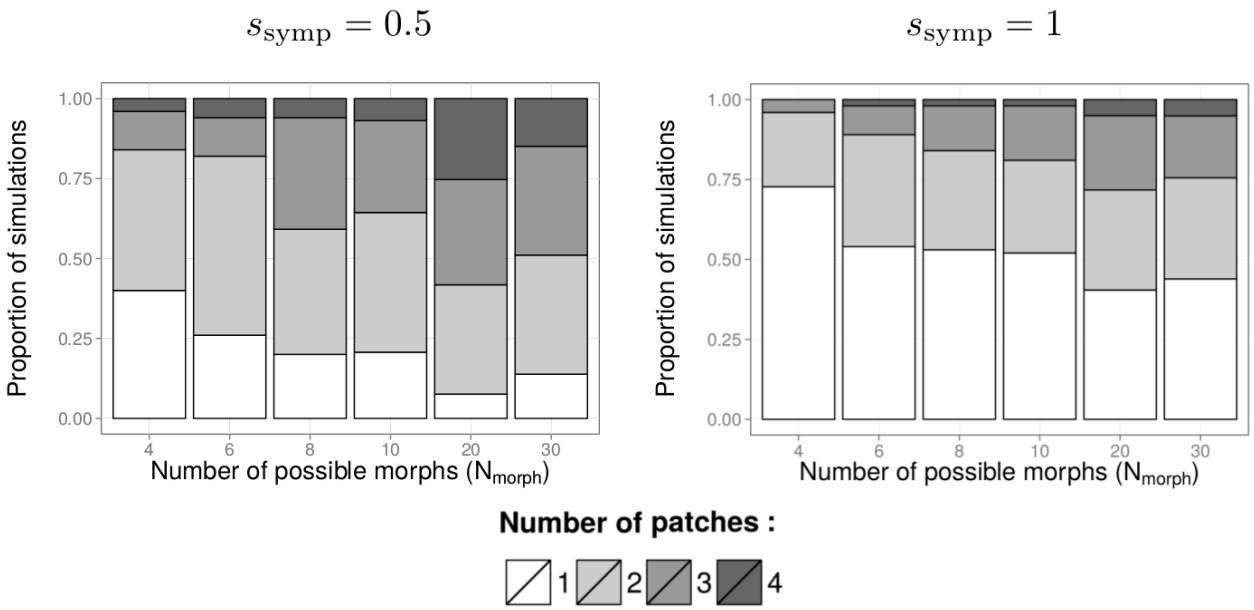


Figure S9: Formation of the spatial mosaic of morphs. We plot the proportion of simulations leading to different numbers of patches in the mosaic (represented by different shades of grey), when speciation is entirely sympatric ($s_{\text{symp}} = 1$), and when speciation is either sympatric or allopatric ($s_{\text{symp}} = 0.5$). Parameter values: see Table 1. $s_c = 0.50$.
*The formation of the mosaic is more likely when speciation can be allopatric ($s_{symp} = 0.5$).*

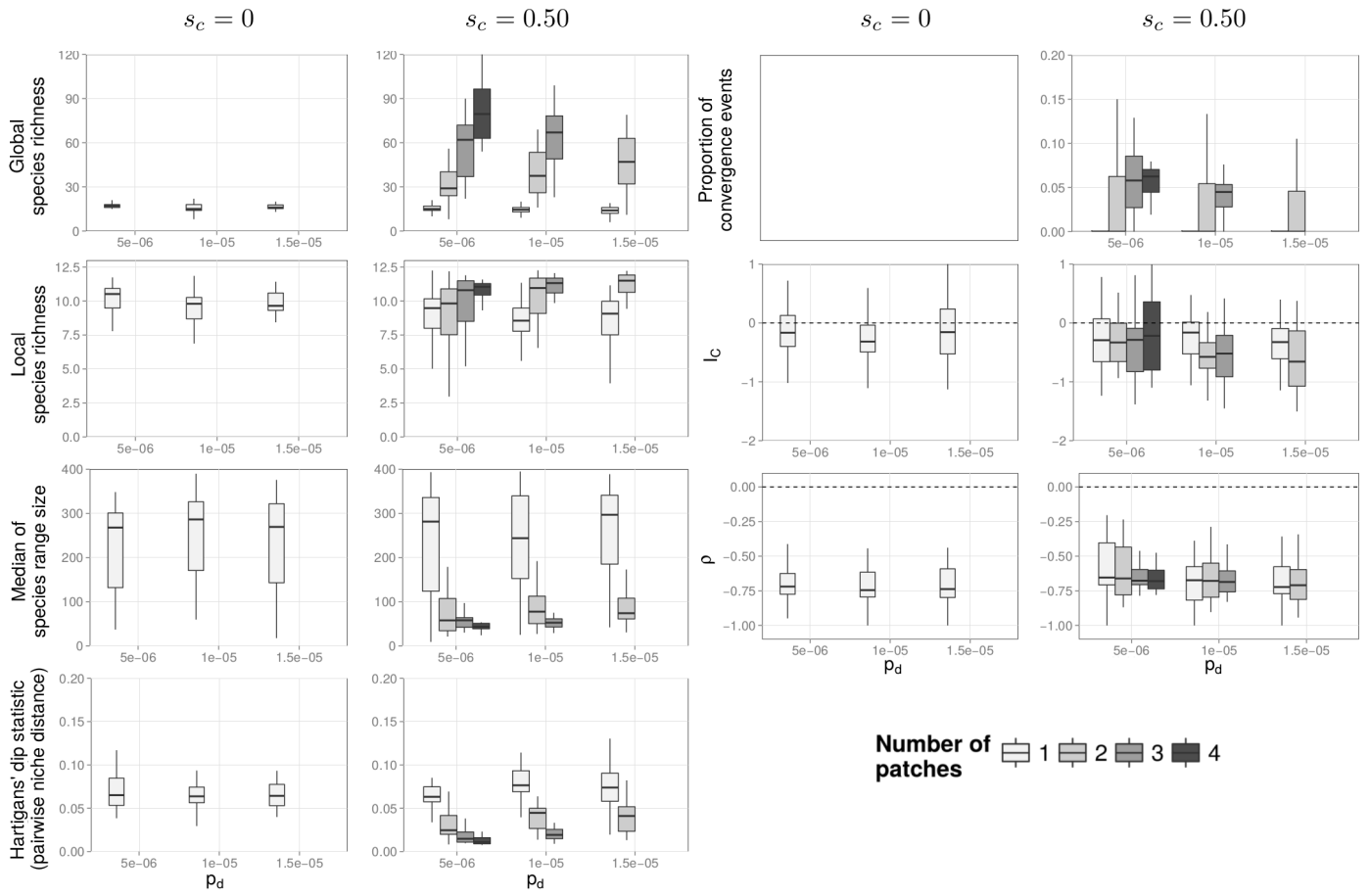


Figure S10: Relationship between the number of patches of the mosaic emerging from the simulations, the spatial and ecological structure of the prey community and the reconstructed phylogeny. Effects of the **probability of cell destruction in any given cell** ($\mathbf{p_d}$). From top to bottom, we plot the diversity of the simulated clades (global and local species richnesses), the geography of species (median of species range size), species niche occupation (Hartigans' dip statistic of the distribution of pairwise niche distance), the proportion of convergence events, the estimator of the imbalance $I_C$ of the resulting trees using Colless' index, and the temporal shift in diversification rate $\rho$. For each combination of parameters, simulations are classified according to the number of patches of their resulting mosaics (different shades of grey). Data distribution is represented by box-and-whiskers plot. Parameter values: see Table 1.
*Increasing the probability of cell destruction (high $p_d$) inhibits the formation of the spatial mosaic (Fig. S5), because it reduces the effective speciation rate with colour shift. This effect on the spatial mosaic affects the macroevolutionary pattern (lower species richnesses, larger species ranges, less balanced phylogenies, more convergence events observed, when the number of patches is low). Direct and indirect (through the formation of the mosaic) effects of $p_d$ on the macroevolutionary pattern can be redundant – high $p_d$ results in mosaics with a low number of patches (thereby giving little opportunity to observe convergence events in the phylogenies) and favours directly a low proportion of convergence events (lower effective speciation rate with colour shift).*

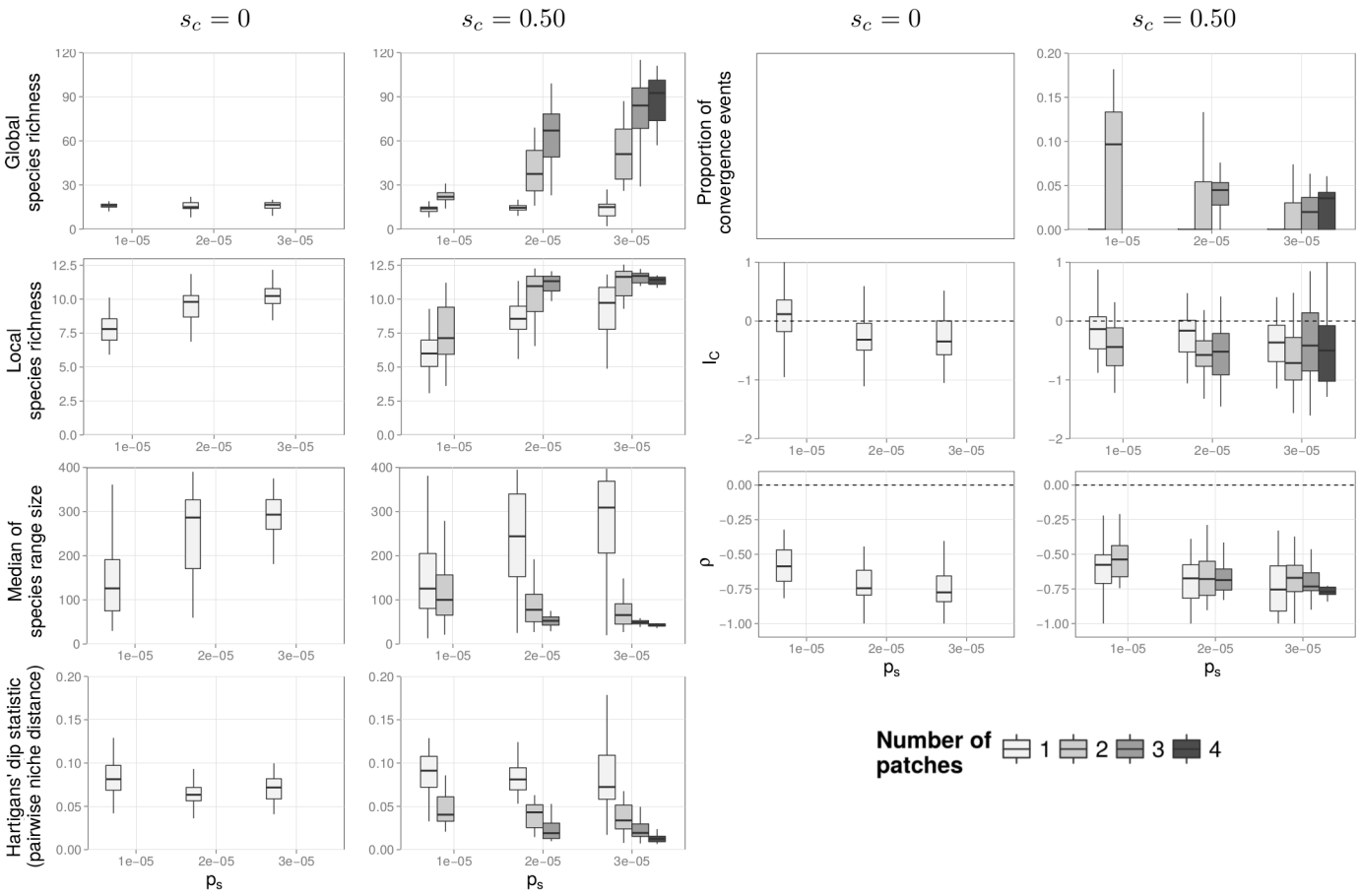


Figure S11: Relationship between the number of patches of the mosaic emerging from the simulations, the spatial and ecological structure of the prey community and the reconstructed phylogeny. Effects of the **probability of speciation of each species in any given cell** ($\mathbf{p_s}$). From top to bottom, we plot the diversity of the simulated clades (global and local species richnesses), the geography of species (median of species range size), species niche occupation (Hartigans' dip statistic of the distribution of pairwise niche distance), the proportion of convergence events, the estimator of the imbalance $I_C$ of the resulting trees using Colless' index, and the temporal shift in diversification rate $\rho$. For each combination of parameters, simulations are classified according to the number of patches of their resulting mosaics (different shades of grey). Data distribution is represented by box-and-whiskers plot. Parameter values: see Table 1.
*Increasing the probability of speciation (high $p_s$) favours the formation of the spatial mosaic (Fig. S5), because it increases the effective speciation rate with colour shift. This effect on the spatial mosaic affects the macroevolutionary pattern (higher species richnesses, smaller species ranges, more balanced phylogenies, more convergence events observed, when the number of patches is high). Direct and indirect (through the formation of the mosaic) effects of $p_s$ on the macroevolutionary pattern can be redundant – increasing $p_s$ both results in mosaics with high numbers of patches (and therefore have a positive impact on global species richness) and increases local species richness; or antagonistic – increasing $p_s$ results in mosaics with high numbers of patches (giving more opportunities to observe convergence), but inhibits convergence (higher effective speciation rate without colour shift – speeding up the invasion of the grid).*

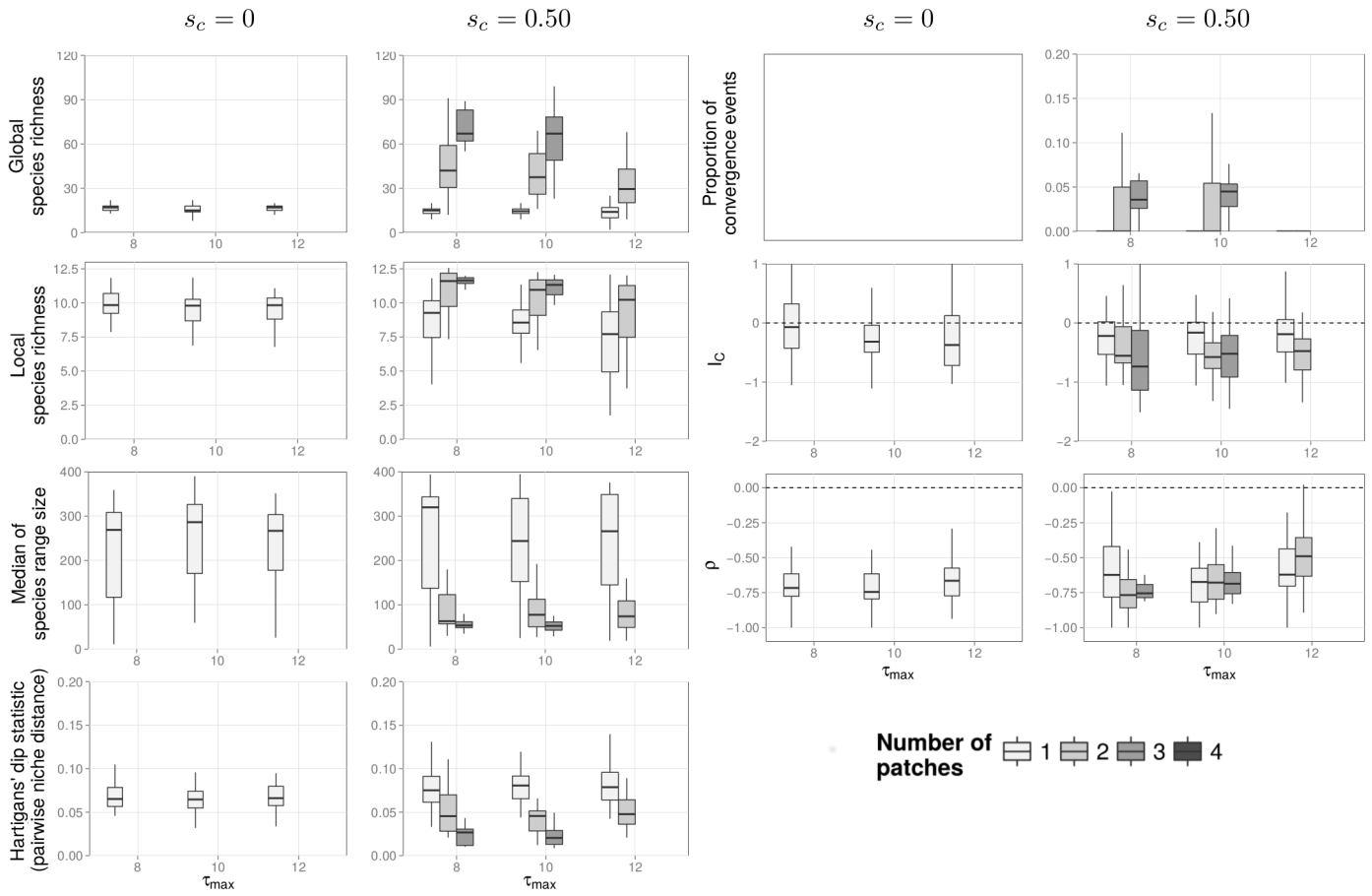


Figure S12: Relationship between the number of patches of the mosaic emerging from the simulations, the spatial and ecological structure of the prey community and the reconstructed phylogeny. Effects of the **number of prey attacked before predation on a given morph ceases** ($\tau_{\max}$). From top to bottom, we plot the diversity of the simulated clades (global and local species richnesses), the geography of species (median of species range size), species niche occupation (Hartigans' dip statistic of the distribution of pairwise niche distance), the proportion of convergence events, the estimator of the imbalance $I_{\mathrm{C}}$ of the resulting trees using Colless' index, and the temporal shift in diversification rate $\rho$. For each combination of parameters, simulations are classified according to the number of patches of their resulting mosaics (different shades of grey). Data distribution is represented by box-and-whiskers plot. Parameter values: see Table 1.
*Increasing or decreasing the number of prey attacked before predation on a given morph ceases ($\tau_{max}$) inhibits the formation of the spatial mosaic (Fig. S5), because it increases the effective speciation rate without colour shift – speeding up the invasion of the grid –, or decreases the effective speciation rate with colour shift, respectively. This effect on the spatial mosaic affects the macroevolutionary pattern (lower species richnesses, larger species ranges, less balanced phylogenies, more convergence events observed, when the number of patches is low).*

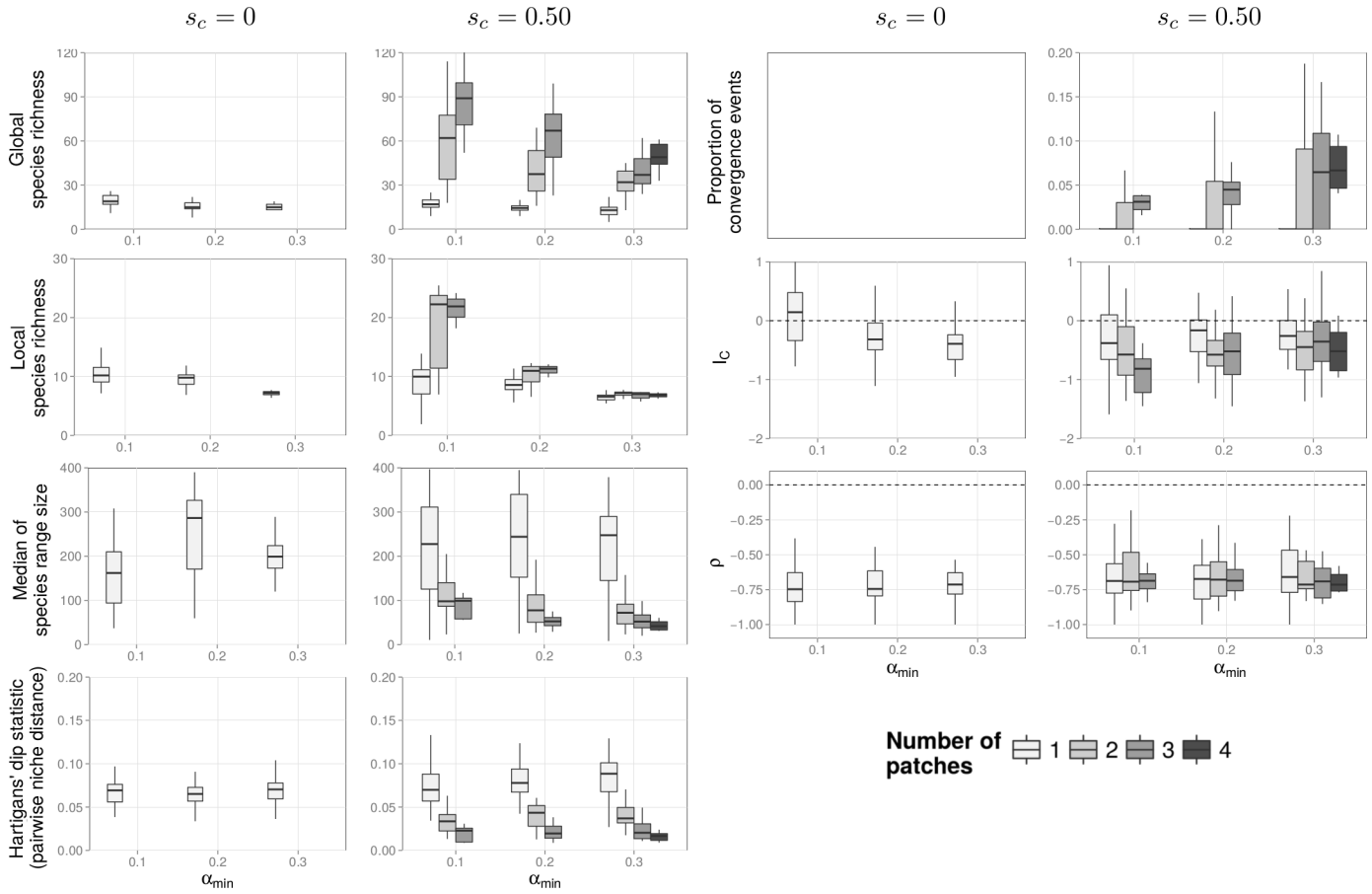


Figure S13: Relationship between the number of patches of the mosaic emerging from the simulations, the spatial and ecological structure of the prey community and the reconstructed phylogeny. Effects of the **minimum competition term possible** ($\alpha_{\min}$) (see figure S2B). From top to bottom, we plot the diversity of the simulated clades (global and local species richnesses), the geography of species (median of species range size), species niche occupation (Hartigans' dip statistic of the distribution of pairwise niche distance), the proportion of convergence events, the estimator of the imbalance $I_C$ of the resulting trees using Colless' index, and the temporal shift in diversification rate $\rho$. For each combination of parameters, simulations are classified according to the number of patches of their resulting mosaics (different shades of grey). Data distribution is represented by box-and-whiskers plot. Parameter values: see Table 1.

*Increasing the minimum competition term possible (high $\alpha_{min}$) favours the formation of the spatial mosaic (Fig. S5), because it decreases the effective speciation rate without colour shift – slowing down the invasion of the grid. This effect on the spatial mosaic affects the macroevolutionary pattern (higher species richnesses, smaller species ranges, more balanced phylogenies, more convergence events observed, when the number of patches is high). Direct and indirect (through the formation of the mosaic) effects of $\alpha_{min}$ on the macroevolutionary pattern can be redundant – increasing $\alpha_{min}$ favours the formation of the spatial mosaic (giving more opportunities to observe convergence), and favours directly convergence events; or antagonistic – increasing $\alpha_{min}$ favours the formation of the spatial mosaic, which has a positive impact on global species richness, but decreases local species richness.*

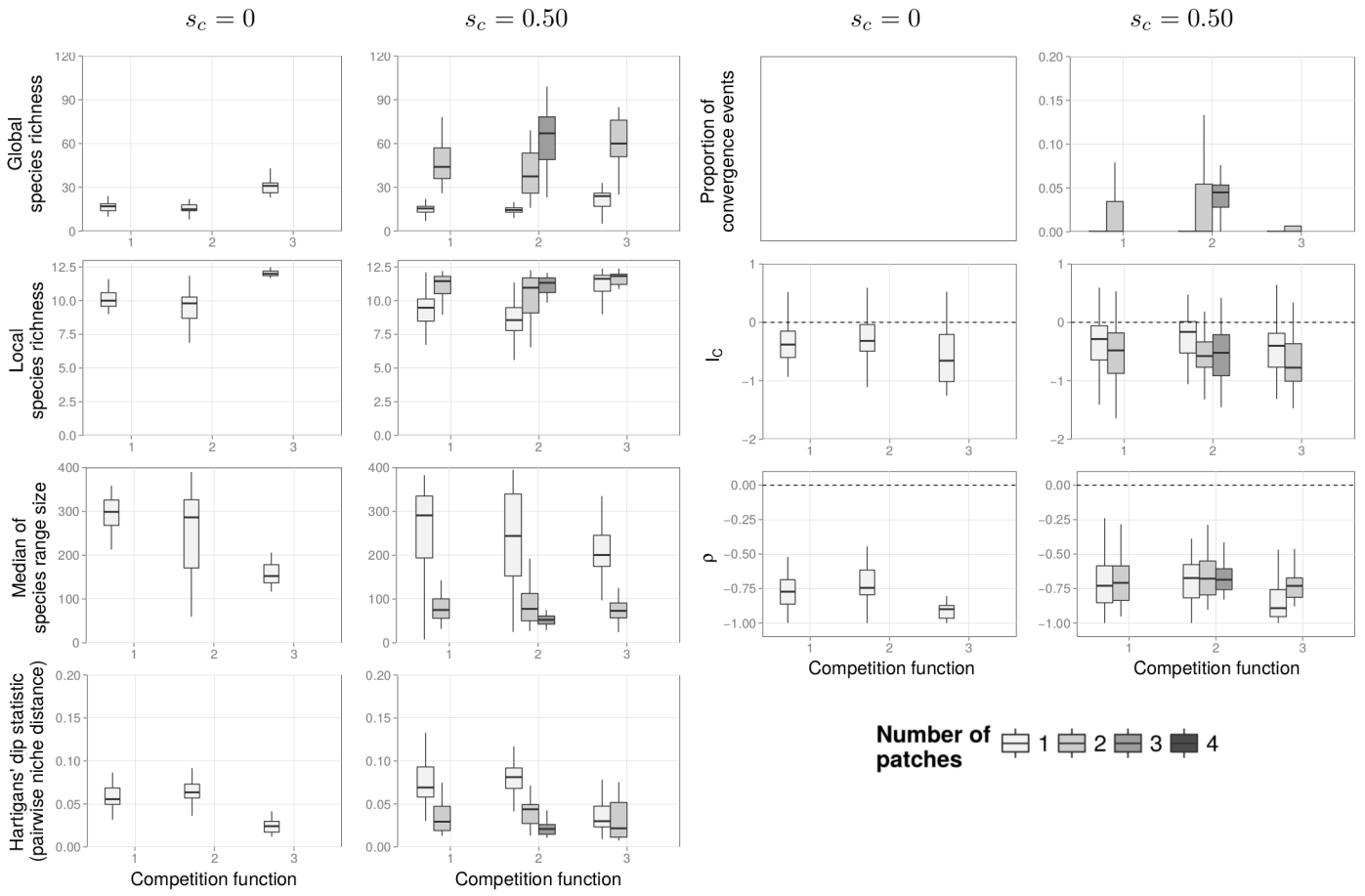


Figure S14: Relationship between the number of patches of the mosaic emerging from the simulations, the spatial and ecological structure of the prey community and the reconstructed phylogeny. Effects of the **competition function** (see figure S2A). From top to bottom, we plot the diversity of the simulated clades (global and local species richnesses), the geography of species (median of species range size), species niche occupation (Hartigans' dip statistic of the distribution of pairwise niche distance), the proportion of convergence events, the estimator of the imbalance $I_{\mathrm{C}}$ of the resulting trees using Colless' index, and the temporal shift in diversification rate $\rho$. For each combination of parameters, simulations are classified according to the number of patches of their resulting mosaics (different shades of grey). Data distribution is represented by box-and-whiskers plot. Parameter values: see Table 1.

*Increasing or decreasing the intensity of competition inhibits the formation of the spatial mosaic (Fig. S5), because it either increases the effective speciation rate without colour shift (Competition function 3) – speeding up the invasion of the grid – , or decreases the effective speciation rate with colour shift (Competition function 1). This effect on the spatial mosaic affects the macroevolutionary pattern (lower species richnesses, larger species ranges, less balanced phylogenies, less convergence events observed, when the number of patches is low).*